Relationships among Multifocal Electroretinogram Amplitude, Visual Field Sensitivity, and SD-OCT Receptor Layer Thicknesses in Patients with Retinitis Pigmentosa

Yuquan Wen,[1] *Martin Klein,*[1] *Donald C. Hood,*[2,3] *and David G. Birch*[1,4]

Purpose. To compare local functional measures, the multifocal electroretinogram (mfERG) and visual field sensitivity, with a local structural measure, spectral domain (SD) optical coherence tomography (OCT), of receptor damage in patients with retinitis pigmentosa (RP).

Methods. MfERGs, visual fields, and SD-OCT scans were obtained from 10 patients with RP, ranging in age from 23 to 59 years. Average amplitudes, average linear sensitivities, and average layer thicknesses were measured from within the central 3° and from three concentric annuli located between 3° and 8°, 8° and 15°, and 15° and 24°. A computer program aided manual segmentation and calculated OCT thickness in the scans.

Results. Within each patient with RP, mfERG amplitude for each circle/annulus was highly correlated with corresponding layer thicknesses in the outer retina ($r = 0.88$ to 0.99), but not at all correlated with thickness of the inner nuclear layer or total retina. Across all ring eccentricities, relative mfERG amplitude and relative visual field sensitivity were correlated with relative SD-OCT outer retinal thickness.

Conclusions. In patients with RP, preserved cone photoreceptor function measured by mfERG amplitude and visual field sensitivity correlate well with the remaining thickness of the photoreceptor layer. All three measures show comparable relative loss beyond 3° eccentricity. In the fovea, SD-OCT outer retina thickness showed less relative loss than either mfERG or visual field sensitivity. (*Invest Ophthalmol Vis Sci.* 2012;53: 833–840) DOI:10.1167/iovs.11-8410

Retinitis pigmentosa (RP) is a group of hereditary retinal degenerations characterized by progressive degeneration of rod and cone photoreceptors.[1] Patients with RP eventually develop tunnel vision with a residual central island of vision preserved in the central 20°.[2] Cone-mediated responses are present in the multifocal electroretinogram (mfERG) from regions with functional photoreceptors.[3–7] Different from full-field ERG, mfERGs can be recorded from many retinal regions during a single recording.[8] Since the introduction of the mfERG in 1992,[8] numerous studies have examined the relationships between local mfERG responses and other measures of visual function in patients with RP. For example, a significant correlation was found between visual acuity and amplitude of the central segment of the mfERGs.[9] In mild RP, summed mfERG amplitude in outer rings strongly correlated with the full-field ERG mixed cone-rod response amplitude.[9] Moreover, good correlation was found between sensitivity measured with standard automated perimetry and mfERG amplitudes and implicit time.[10–12] In some RP patients with good visual acuity, high-density fundus autofluorescence (AF) correlates well with mfERG amplitudes.[13] As early as 2003, adding mfERG and time-domain optical coherence tomography (OCT) to clinical eye examinations was proposed for a more refined evaluation of visual function in patients with RP.[14,15] However, it was not until the emergence of spectral domain (SD)-OCT that investigations into the relationships between layer thicknesses and functional measures became possible. In this study, we asked whether a significant correlation exists between receptor layer thickness and mfERG, and whether this correlation, if it exists, is similar to what was reported previously between OCT layer thicknesses and visual field sensitivity.[16,17]

Materials and Methods

Patients

Ten patients with RP and 10 individuals with normal vision participated this study. The patients with RP were referred to the Retina Foundation of the Southwest (RFSW) by ophthalmologists specializing in retinal diseases. Genetic testing results were retrieved from the database of the Southwest Eye Registry of the RFSW. Patients ranged in age from 23 to 59 years (41 ± 15 years, mean ± SD). Patients were selected who had visual acuity (VA) equal or better than 20/32, fields at least 20° in diameter, and foveal sensitivity within 5 dB of mean normal. Patients with cystoid macular edema (CME) or high myopia (higher than 6.00 diopters) were not included in this study. Ten individuals with normal eye findings served as control. The tenets of the Declaration of Helsinki were followed and all individuals gave written informed consent after a full explanation of the tests and procedures. All procedures were approved by the University of Texas Southwestern (UTSW) institutional review board.

Clinical Examination

For each patient, best-corrected visual acuity was measured with the electronic visual acuity (EVA) tester using the electronic Early Treatment for Diabetic Retinopathy Study (E-ETDRS) protocol.[18] Central

From the [1]Retina Foundation of the Southwest, Dallas, Texas; Departments of [2]Psychology and [3]Ophthalmology, Columbia University, New York, New York; and [4]Department of Ophthalmology, UT Southwestern, Dallas, Texas.

Supported by National Institutes of Health Grant NEI R01 09076 (DGB, DCH) and the Foundation Fighting Blindness.

Submitted for publication August 12, 2011; revised November 14, 2011; accepted December 27, 2011.

Disclosure: **Y. Wen**, None; **M. Klein**, None; **D.C. Hood**, Topcon Medical Systems (F, C); **D.G. Birch**, None

Corresponding author: Yuquan Wen, 9900 N Central Expressway, Suite 400, Dallas, TX 75231; ywen@retinafoundation.org.

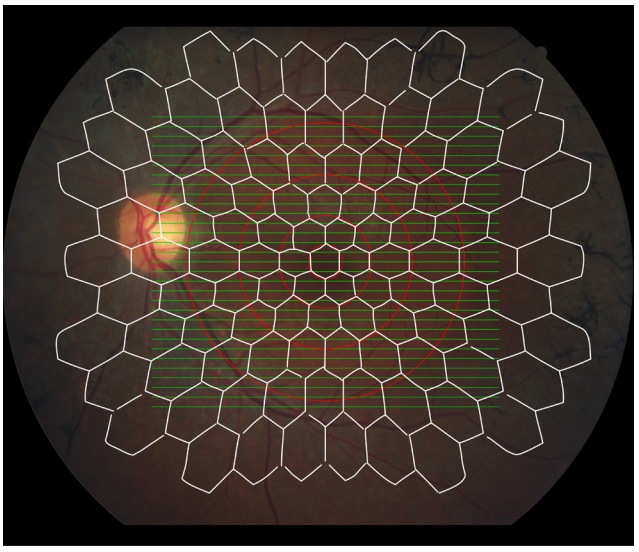

FIGURE 1. SD-OCT volume scans (30° × 25°, 31 B-scans, *green*) overlaid with stimulus pattern of 103 scaled hexagons covering the central 50° (Veris [EDI] mfERG, *white*) in a patient with RP. The correlation between SD-OCT and mfERG was performed in four concentric ring/annuli (central 3°, 3°–8°, 8°–15°, 15°–24°, *red*) around the fovea center.

visual fields were estimated using a visual field analyzer (Humphrey Visual Field Analyzer; 30–2 SITA Fast protocol; Humphrey Instruments, San Leandro, CA). Summed visual field sensitivity (in linear units) was calculated for four regions (central 3°, 3°–8°, 8°–15°, 15°–24°). Dark-adapted thresholds were measured with a dark-adaptometer (Goldmann-Weekers; Haag-Streit, Köniz, Switzerland), using an 11° achromatic test target located 7° inferior to fixation after pupil dilation (tropicamide 1.0% and phenylephrine 2.5%) and 45-minute dark adaptation. Subsequently, full-field electroretinograms (ffERGs) were recorded using the International Society for Clinical Electrophysiology of Vision (ISCEV) standard protocol.[19]

MfERG Stimulus, Recording, and Analysis

All patients demonstrated good signal to noise ratios for mfERGs recorded within the central 8°. Procedures for recording mfERGs have been described in our previous publications[10,20–22] and conform to ISCEV guidelines.[23] Briefly, differential signals were acquired, amplified, and analyzed using a commercial mfERG system (Veris Science 5.1.10X; EDI, Redwood City, CA). A corneal electrode (Burian-Allen; Hansen Labs, Coralville, IA) was used to collect differential signals from the corneal surface. An ear clip electrode was used as ground. The signal was amplified at gain of 100,000 and filtered between cutoff frequencies of 10 to 300 Hz. Stimuli were projected to the central 50° of the retina using the 103 scaled hexagon display, which had a mean luminance of 100 cd/m^2 and contrast ≥ 90%. Patient's fixation was actively monitored during each segment of recording using an infrared fundus camera. Only first-order kernel response was used for analysis. As shown in Figures 1 and 2, summed responses in four concentric ring/annuli (central 3°, 3°–8°, 8°–15°, and 15°–24°) were derived using software (Veris Science; EDI).

SD-OCT Image Acquisition and Analysis

The SD-OCT imaging was performed (Spectralis HRA-OCT, version 5.3.3.0; Heidelberg Engineering, Heidelberg, Germany). The automatic real-time (ART) eye tracking software on the OCT imager (Spectralis; Heidelberg Engineering) enables real-time eye tracking. As shown in Figure 1, the volume scan protocol (high-speed mode) covered the central retina (30° × 25°) with 31 line scans that were 30° in length. Each line scan represents the average of 15 images. These 31 line scan images were exported into tagged image file format (TIFF) from the OCT imager (Spectralis HRA-OCT; Heidelberg Engineering), which also provides the scales (μm/pixel) for these images. Software subroutines (based in Igor Pro 6.12; WaveMetrics, Inc., Lake Oswego, OR) were written to aid in segmentation

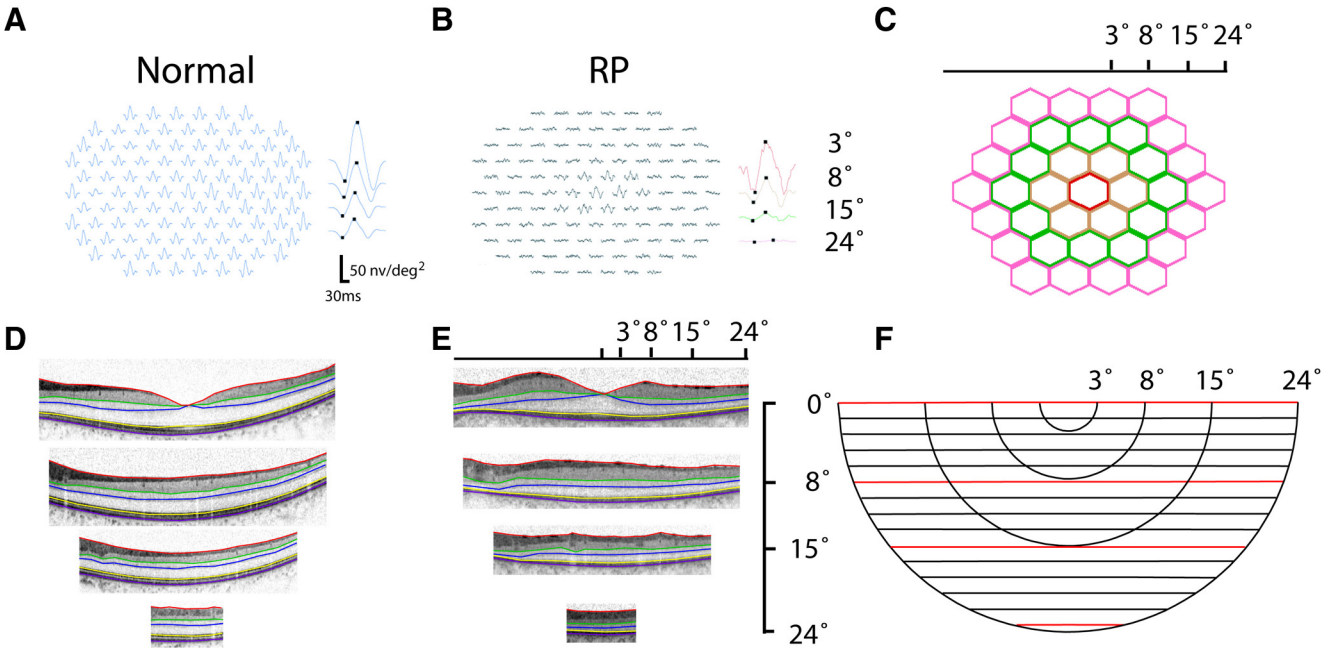

FIGURE 2. (**A**) MfERG recording in a normal individual and (**B**) a patient with RP (**C**). Responses were summed from four rings (central 3°, 3°–8°, 8°–15°, 15°–24°), which are represented by color-coded hexagon groups. (**D**) SD-OCT image in a normal individual and (**E**) a patient with RP were tailored to the limit of a 24° circle before segmentation. (**F**) SD-OCT volume scan overlaid with segmentation lines (*red*) at horizontal meridian (0°), and 8°, 15°, and 24° inferior to the horizontal meridian.

and to calculate total and layer thicknesses in four concentric ring/annuli (central 3°, 3°–8°, 8°–15°, and 15°–24°) around the fovea center (Figs. 1, 2). These four concentric circle/annuli matched the inner four concentric circle/annuli in the mfERG (Fig. 1). The software calculates the intersections of these four ring/annuli with 31 line scans using parameters provided by the OCT imager (Spectralis HRA-OCT; Heidelberg Engineering), including scales of OCT images (μm/pixel), pixel numbers, scan angle (30°), and distance between B-scans (Fig. 2). Pixels outside of the 24° circle were cropped by the program so that only OCT images within the 24° circle were preserved for subsequent manual segmentation (Fig. 2). The manual segmentation approach and strategy were comparable to the software developed by Hood et al.[24] (Matlab-based; MathWorks, Natick, MA). After all segmentation lines were drawn, the software calculated the average OCT thicknesses in the four concentric circle/annuli around fovea center. The OCT thicknesses reported include outer segment (OS)+, REC+ (RPE, photoreceptor outer segment, inner segment, outer nuclear layer, and outer plexiform layer), outer nuclear layer (ONL), inner nuclear layer (INL), and TR (total retina: neural retina + RPE) thicknesses.[24] The OS+ thickness was measured from distal border of RPE/Bruch's membrane (BM) and choroid [RPE(+BM)/choroid] to the boundary between photoreceptor inner segment (IS) and OS. As in previous work,[17,24] we hypothesize that OS+ thickness includes the photoreceptor OS and a residual constant (b = 21.5 μm). The residual constant (b) primarily consists of RPE and part of the Bruch's membrane, but may also contain a contribution from RPE apical processes and distal tips of the outer segments. The REC+ thickness was measured from the RPE(+BM)/choroid to the border of INL and outer plexiform layer (OPL). ONL thickness indexes the distance from IS/OS junction to distal border of OPL/receptor, which comprises photoreceptor inner segments, photoreceptor nuclei, the fibers of Henle, and OPL.[25] OS × ONL represents the product of OS and ONL thickness.[17] INL thickness represents thickness of the INL, which is enveloped between the distal border of OPL/receptor and the border between the INL and the inner plexiform/ganglion cell layer. TR thickness includes the thickness of neural retina plus the thickness of the RPE and part of the BM, which covers the thickness between the RPE(+BM)/choroid and the border between the vitreous and retinal nerve fiber layer.

Strategy to Correlate MfERG Results with OCT Findings

Figure 1 shows the retinal area covered by the OCT volume scan (green lines) and mfERG stimulus pattern (white hexagons). The 31 B-scans (volume scan protocol) extends 30° nasal-to-temporal and 25° superior-to-inferior around the foveal center, which fully covers the central four hexagon rings in the mfERG stimulus pattern. The four concentric red circles around the fovea (3°, 8°, 15°, and 24°) indicate the spatial correspondence of areas covered by SD-OCT B-scans and mfERG stimuli (and visual fields). Average thicknesses (OS+, REC+, ONL, INL, and TR thickness) summed from these loci (central 3°, 3°–8°, 8°–15°, 15°–24°) were correlated with mfERG amplitudes and field sensitivity summed in respective regions.

Results

Patient Characteristics

Table 1 shows clinical and genetic findings in the patients. The 10 patients with RP ranged in age from 23 to 59 years (41 ± 15 years, mean ± SD), including 4 autosomal dominant (ad)RP and 6 recessive/isolate RP. Genetic testing revealed mutations in rhodopsin (RHO) (one case) and peripherin/RDS (one case) in the patients with adRP. Best-corrected visual acuity was better than 20/32. All patients had best-corrected visual acuity better or equal to 20/32 and a visual field extending beyond 20° (Table 1). Foveal sensitivity ranged from 34 to 39 dB (36 ± 2 dB, mean ± SD). The mean dark adapted threshold was 3.0 ± 0.9 log microapostilbs in these patients, which was above the normal limit of 1.75 ± 0.25 log microapostilbs.[26] The ISCEV rod response ranged from nondetectable to 38 μV (16 ± 15 μV), all below the normal lower limit.[26] In comparison, cone function was better preserved.

Reduced Layer Thicknesses and MfERG Amplitudes in Patients with RP

Figure 2 shows representative mfERG responses and SD-OCT layer thickness measurements in a normal individual and a patient with RP. Compared with normal (Fig. 2A), most individual responses in the periphery in RP (Fig. 2B) were diminished or nonexistent. The summed responses (central 3°, 3°–8°, 8°–15°, and 15°–24°) were shown next to the individual responses (Figs. 2A, 2B). The four rings of hexagons used to derive the summed responses were shown in four distinct colors for clarification (Fig. 2C). Representative segments of OCT scans (horizontal meridian, 8°, 15°, and 24°) in a normal individual (Fig. 2D) and a patient with RP (Fig. 2E) are shown for comparison. Their corresponding locations in the volume scan are shown in red in Figure 2F. This patient shows relatively intact outer retinal thickness within the central 8° with a precipitous decline in OS+, REC+, and ONL thickness more eccentrically.

Figures 3A–D shows thicknesses of the OS+, REC+, INL, and TR layers for the 4 ring eccentricities. The average values ± 1 SE for the normal controls (large filled circle) and patients (large open circle) are shown next to the data for the individual patients (small open symbols). Statistical comparisons of the thicknesses in RP (open symbols) and normal (filled symbol) are also shown in Table 2. Significant reductions ($P \leq 0.01$) were found in OS+ thickness in each of the four regions in patients with RP comparing with normal (Fig. 3A, Table 2). For REC+ thickness, significant reductions ($P < 0.001$) were found at 3°–8°, 8°–15°, and

Table 1. Clinical Findings in Patients with RP

Patient Number	Eye	Age (y)	Type	VA	Extent of Central Field (°)	Foveal Sensitivity (dB)	DA (log)	Rod Amplitude (μV)	LA 31Hz (μV)
652	OD	59	adRP/RHO (Pro23His)	20/32	20	37	3.7	ND	2.4
4740	OS	26	adRP	20/25	20	34	3.2	ND	1.8
5931	OS	58	adRP/(RDS)	20/25	60	37	2.4	38	52.4
7222	OS	46	Recessive	20/32	20	39	4.3	ND	2.6
7808	OS	59	Recessive	20/25	20	35	3.7	4	94.7
8438	OS	23	Recessive	20/25	40	36	2.1	9	11.6
9944	OS	40	Isolate	20/20	30	35	2.0	14	22.3
9958	OS	23	Isolate	20/20	30	38	3.0	ND	10.5
10244	OS	31	Isolate	20/25	20	35	4.0	ND	0.7
10413	OD	48	adRP	20/25	30	35	1.7	ND	2.6
Normal[26]				≥20/20	>60	39	<2.0	>92	>42

DA, visual threshold (11° test) after 45-minute dark adaption; LA 31Hz, light-adapted cone 31 Hz ERG response amplitudes; ND, not detectable.

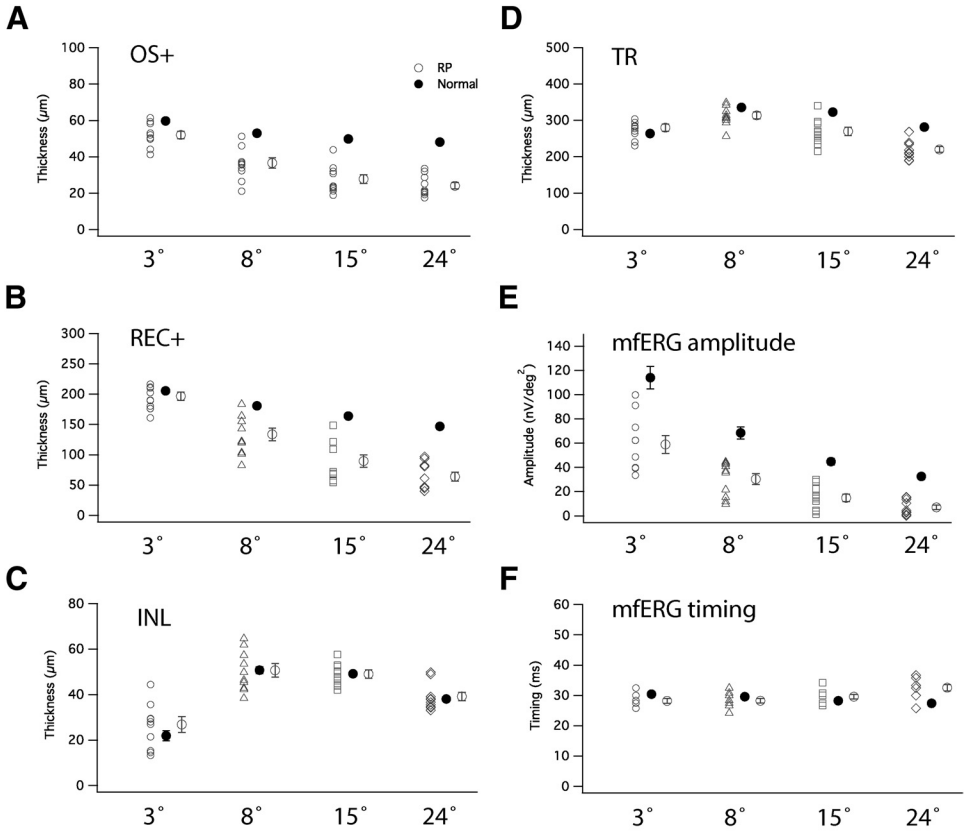

FIGURE 3. (**A–D**) Scatter plots of thicknesses of OS+, REC+, INL, and TR measured in central 3°, 3°–8°, 8°–15°, and 15°–24°. *Filled symbols*, normal individuals. *Open symbols*, patients with RP. Average values (*larger symbols*) with SE are shown to the right of the group of plots. (**A**) OS+ thicknesses in patients with RP were significantly shorter than normal in all loci. (**B**) REC+ thicknesses in patients with RP were significantly shorter than normal in all loci except the central 3°. (**C**) INL thickness did not differ in patients versus normal control. (**D**) TR thickness was not shorter than normal in the central 3° and 3°–8°, but was shorter in two other loci. (**E–F**) MfERG amplitude and implicit time in patients with RP and normal controls. MfERG amplitudes in RP were shorter than normal in all four loci, but longer than normal implicit time in RP was limited to 15°–24°.

15°–24°, but not in the central 3° ($P = 0.33$) (Fig. 3B, Table 2). No difference was detected in INL thicknesses in any of the four regions between RP and normal (Fig. 3C, Table 2). Significant reductions ($P < 0.05$) in TR thicknesses were only found at 8°–15°, and 15°–24°, but not in the central 3° and 3°–8° (Fig. 3D, Table 2). Table 2 shows that thickness reductions in patients with RP ranged from 13% to 50% in OS+ thickness and from 4% to 56% in REC+ thickness.

Figure 3E shows the distribution of mfERG amplitudes in 10 patients with RP and 10 normal control subjects. Average amplitudes were reduced 48%, 56%, 67%, and 78% at the central 3°, 3°–8°, 8°–15°, and 15°–24° respectively in patients with RP compared with normal average ($P < 0.001$). Figure 3F shows P1 implicit time in the 10 patients with RP and the normal average. Mean implicit time was delayed 19% compared with normal between 15°–24°, which is statistically significant ($P < 0.001$).

The Segmented OCT Thicknesses are Correlated with MfERG Measures

In normal subjects, both average mfERG amplitude and average REC+ thickness were greatest in the fovea and declined monotonically with eccentricity. Figure 4 shows means and standard

TABLE 2. Segmented SD-OCT Thicknesses (Mean ± SE) in 10 Patients with RP and 10 Normal Individuals

	OS+ (μm)	REC+	INL	TR
RP				
3°	52 ± 2	197 ± 7	27 ± 3	280 ± 10
Change % (*P*)	−13* (0.01)	−4 (0.33)	23 (0.25)	6 (0.18)
3°–8°	37 ± 3	134 ± 10	51 ± 3	314 ± 10
Change % (*P*)	−30† (<0.001)	−26† (0.0005)	0	−6 (0.07)
8°–15°	28 ± 2	90 ± 11	49 ± 2	270 ± 11
Change % (*P*)	−44† (<0.001)	−45† (<0.001)	0	−16† (0.0007)
15°–24°	24 ± 2	64 ± 7	39 ± 2	220 ± 8
Change % (*P*)	−50† (<0.001)	−56† (<0.001)	0	−22† (<0.001)
Normal				
3°	60 ± 1	206 ± 2	22 ± 2	264 ± 5
3°–8°	53 ± 1	181 ± 1	51 ± 2	335 ± 5
8°–15°	50 ± 1	164 ± 2	49 ± 1	323 ± 5
15°–24°	48 ± 1	147 ± 2	38 ± 1	282 ± 4

* $P < 0.05$ when compared with normal.
† $P < 0.001$ when compared with normal.

errors for both measures at each ring. A linear fit provided a reasonable description of the data, with $r = 0.98$; $P = 0.016$ for REC+ thickness (Fig. 4).

In Figure 5, functions relating REC+ thickness to mfERG amplitude are shown for the 10 patients (open symbols) in comparison with the normal results from Figure 4 shown as the filled symbols and dashed line. For each patient, REC+ thickness and mfERG amplitude are positively correlated across the 4 retinal regions (open symbols, linear fit in gray). Table 3 lists Pearson's correlation coefficient (r) and statistical significance (P) between mfERG amplitude and OS+, REC+, INL, or TR for all patients with RP. Each of the 10 patients showed a statistically significant correlation ($P \leq 0.01$) between REC+ thickness and corresponding mfERG amplitudes, with Pearson's correlation coefficient (r) ranging from 0.92 to 0.99 (Table 3). Patient functions were, in general, steeper than the normal function. Relative thickness in the fovea was minimally reduced below normal, while foveal mfERG amplitudes were substantially lower than normal in most patients.

Nine out of 10 patients also showed a significant correlation ($P \leq 0.05$) between OS+ thickness and mfERG amplitudes, with r ranging from 0.88 to 0.99 (Table 3). No significant correlations were observed between mfERG amplitudes and INL or TR thicknesses. These results demonstrate that mfERG amplitudes are highly correlated with layer thicknesses in outer retina in patients with RP, and not at all correlated with thickness of the INL and TR. The implicit time of mfERG in patients with RP did not show a significant correlation with REC+ thickness. However, it is not clear what structural changes should correlate with the implicit time of mfERG.

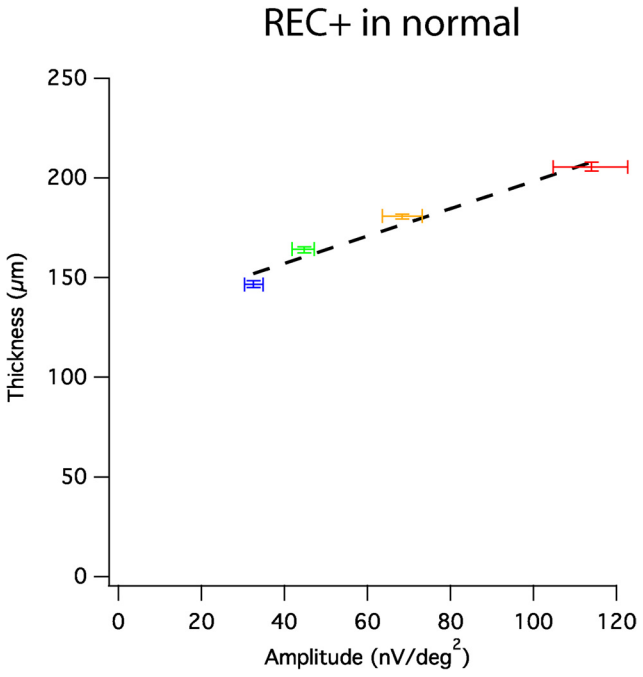

Figure 4. REC+ thickness versus mfERG amplitudes in corresponding loci (mean ± SE). *Horizontal error bars* represent SE for mfERG amplitude; *vertical error bars* represent SE for thickness measures. Significant positive correlations were found ($r = 0.98$, $P = 0.016$). Linear regression (*black broken lines*) provided reasonable descriptions for the positive correlation. *Red*, central 3°; *yellow*, 3°–8°; *green*, 8°–15°; *blue*, 15°–24°.

Relationships among MfERG Amplitude, Visual Field Sensitivity, and Receptor Layer Thickness in Patients with RP

We next sought to determine the relative sensitivity of the three measures (mfERG amplitude, visual field sensitivity, and receptor layer thickness) to retinal degeneration in RP. We used OS × ONL thickness to index the receptor layer thickness changes because it reflects both changes in photoreceptor outer segment length and photoreceptor nuclear layer thickness. Figure 6 shows normalized OS × ONL thickness (open circle), normalized mfERG amplitude (filled circle), and normalized field sensitivity (triangle) for each of the four rings (central 3°, 3°–8°, 8°–15°, and 15°–24°) in the 10 patients with RP. One-way analysis of variance (ANOVA) suggest that these three indices are equally effective in characterizing photoreceptor degeneration in these patients with RP at 3°–8°, 8°–15°, and 15°–24° ($P \geq 0.05$), but not in the central 3° ($P = 0.008$). In the central 3°, normalized mfERG amplitude showed a larger reduction (28% more reduction, $P = 0.007$, paired t-test) than normalized OS × ONL within the central 3°. Normalized field sensitivity showed an almost equivalent relative loss to normalized mfERG amplitude in the central 3°. Thus, these three indices agree well in all regions except that functional measures showed larger loss than SD-OCT layer thickness in the central 3°. In contrast, paired t-tests suggest that mfERG amplitudes showed less reduction than normalized OS × ONL thickness in periphery (8°–15°, and 15°–24°) (Fig. 6).

Discussion

Our goal in this study was to compare functional measures (mfERG and visual field) to structural measures (SD-OCT) in retinitis pigmentosa. To do this, we developed a novel three-dimensional approach so that average ERG amplitudes, average visual sensitivities, and average layer thicknesses could be compared from corresponding retinal regions. These comparisons revealed highly significant positive relationships, especially when REC+ thickness was correlated with mfERG amplitudes in each individual patient (Table 3, Fig. 5).

OS+ and REC+ thickness decreased to an asymptote of approximately 20 and 50 μm, respectively, in regions where the mfERG response was nondetectable. This agrees with our previous findings[17] in patients where field sensitivity was decreased by greater than 10 dB. The residual value of approximately 20 μm consists primarily of RPE(+BM) thickness with a possible contribution from outer segment tips.[17] The REC+ baseline value at 50 μm presumably reflects the residual thickness of RPE(+BM), outer-limiting membrane, outer nuclear layer debri, and outer-plexiform layer. Based on SD-OCT line scans on the horizontal meridian, we previously reported that thinning of the OS layer occurred before thinning of ONL+ in the transitional zone.[25] This conclusion holds for volume scans in the present study, which showed a significant decrease of 13% in OS+ thickness in the central 3° without significant decrease in REC+ thickness (Fig. 3, Table 2). The degree of loss is comparable for OS+ and REC+ at 3°–4°. This is not surprising because the most significant difference in layer thickness measures between histology and SD-OCT lies in the central 3°, where Henle fibers occupy a large portion in the REC+ thickness and is not susceptible to change in RP.[27] As a result, change in REC+ thickness in the central 3° are less sensitive to degeneration than OS+ thickness. This can also explain why normalized mfERG amplitude showed larger reduction in the central 3° than either REC+ (Fig. 3) or normalized OS × ONL in the central 3° (Fig. 6).

In our earlier studies, we showed normalized OS+ and REC+ thicknesses were linearly correlated with the total devi-

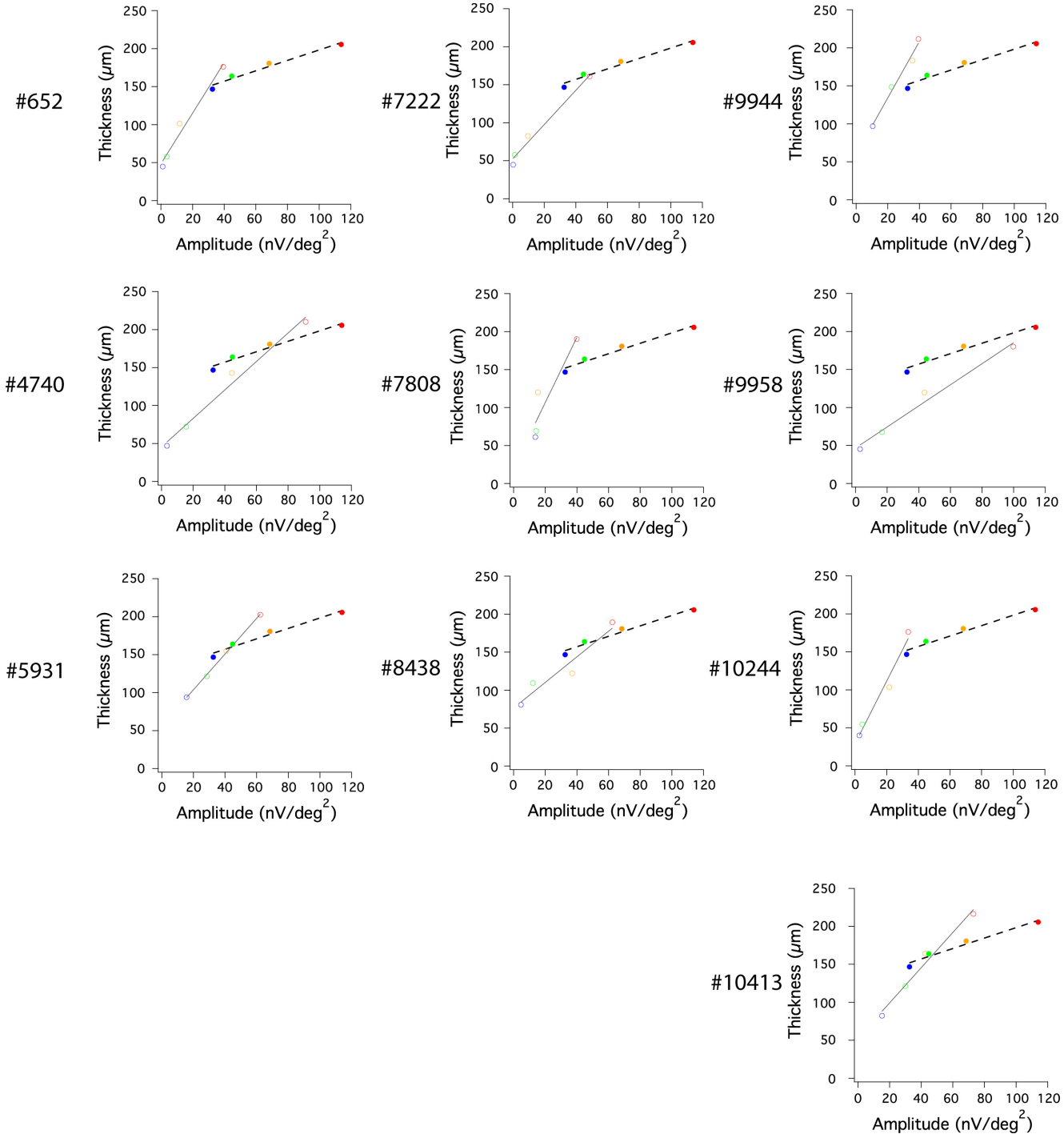

Figure 5. Significant correlation between REC+ thickness and mfERG amplitude in corresponding loci (color-coded) in each of the 10 patients with RP (*unfilled symbols*). *Gray lines* represent linear fit to these correlations in patients; *black broken lines* show linear fit to normal average (*filled symbols*). *Red*, central 3°; *yellow*, 3°–8°; *green*, 8°–15°; *blue*, 15°–24°.

ation (TD) of visual field sensitivity from normal average.[17] In this study, we showed significant positive correlation between SD-OCT layer thickness in outer retina and mfERG amplitude. Together with the established finding that visual field sensitivity significantly correlates to mfERG in RP,[6,11,28] it appears that visual field sensitivity, mfERG response, and SD-OCT layer thickness in the outer retina are intercorrelated and linearly related. This hypothesis is supported by results shown in Figure 6, where the three methods are equally effective in characterizing photoreceptor degeneration in the central 3°–24° of retina with RP. In the central 3°, mfERG amplitude is a more sensitive index for photoreceptor degeneration than SD-OCT receptor layer thickness because Henle fibers occupied a larger share of space in REC+ thickness than in histology and Henle fibers are not susceptible to change in RP.[27] In periphery (8°–24°), normalized mfERG amplitude is reduced less in RP than normalized SD-OCT layer thickness and field sensitivity. This may be due to the stray light interference in mfERG.[20,29] None of these patients showed mfERG responses with the large amplitudes and significantly

TABLE 3. Correlation between Segmented SD-OCT Thicknesses and Corresponding MfERG Response Amplitudes in 10 Patients with RP

	OS+		REC+		INL		TR	
Patient Number	***r***	***P***	***r***	***P***	***r***	***P***	***r***	***P***
652	0.99	<0.001†	0.99	0.006*	−0.35	0.67	0.68	0.16
4740	0.99	0.005*	0.99	0.004*	−0.49	0.75	0.81	0.09
5931	0.88	0.06	0.99	<0.001†	−0.66	0.83	0.73	0.14
7222	0.98	0.01*	0.99	0.004*	−0.6	0.8	0.46	0.27
7808	0.94	0.03*	0.92	0.04*	−0.95	0.98	0.09	0.45
8438	0.99	0.003*	0.96	0.02*	−0.8	0.89	−0.07	0.53
9944	0.99	0.007*	0.99	0.005*	−0.53	0.76	0.17	0.41
9958	0.98	0.008*	0.99	0.005*	−0.39	0.69	0.49	0.25
10244	0.93	0.04*	0.99	0.007*	−0.63	0.81	0.69	0.16
10413	0.99	0.006*	0.99	0.006*	−0.54	0.77	0.49	0.25

* $P < 0.05$.
† $P < 0.001$.

increased implicit times that have been reported previously in a subset of patients with RP.[30]

Interestingly, the only patient with peripherin/RDS mutation (patient 5931) showed a nonsignificant correlation between OS+ thickness and mfERG amplitude. However, the REC+ thickness was significantly correlated with mfERG amplitude. In addition to patient 5931, the mfERG amplitude measured from three other patients with adRP (including one patient with rhodopsin mutation) and six patients with recessive/isolate RP also were significantly correlated with both OS+ and REC+ thicknesses. Due to the small sample size, the statistical power is not sufficient to allow conclusions about gene mutations or hereditary patterns.

In summary, we found strong positive correlations among mfERG amplitude, visual field sensitivity, and SD-OCT receptor layer thicknesses in patients with RP. These three testing methods have complementary advantages in human testing. In the fovea, the mfERG amplitude and visual field sensitivity are more sensitive indices for photoreceptor degeneration than SD-OCT receptor layer thickness. Outside the fovea (3°–24°), the three methods are equally effective although mfERG amplitude changes are prone to interference from stray light. Practically, SD-OCT analysis using segmentation techniques, mfERG, and visual field analysis provide a powerful combination to identify retinal loci with degeneration early and effectively. Moreover, the combined use of these techniques may be useful for determining therapeutic efficacy in treatment trials for retinitis pigmentosa.

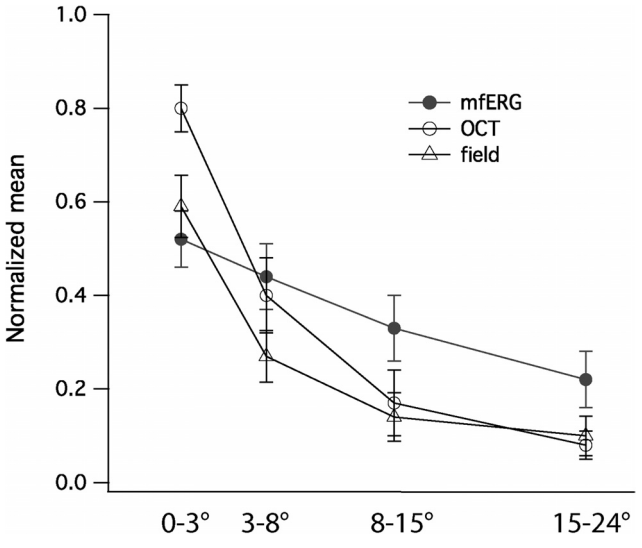

FIGURE 6. Normalized mfERG amplitude, field sensitivity, and receptor layer thickness measure (ONL × OS) in the central 24°. Except in the central 3°, the three indices showed good correspondence in the characterization of photoreceptor degeneration in 10 patients with RP. In the central 3°, normalized mfERG amplitude showed significant larger reduction than SD-OCT thickness. *Filled circle*, mfERG amplitude; *unfilled circle*, SD-OCT measure; *triangle*, visual field sensitivity.

Acknowledgments

The authors thank Dianna Hughbanks-Wheaton and Kaylie Webb at the Southwest Eye Registry and Dr. Stephen Daiger's laboratory at UT Houston for coordinating and performing genetic testing.

References

1. Hartong DT, Berson EL, Dryja TP. Retinitis pigmentosa. *Lancet.* 2006;368:1795–1809.
2. Grover S, Fishman GA, Anderson RJ, Alexander KR, Derlacki DJ. Rate of visual field loss in retinitis pigmentosa. *Ophthalmology.* 1997;104:460–465.
3. Chan HL, Brown B. Investigation of retinitis pigmentosa using the multifocal electroretinogram. *Ophthalmic Physiol Opt.* 1998;18:335–350.
4. Gerth C, Wright T, Heon E, Westall CA. Assessment of central retinal function in patients with advanced retinitis pigmentosa. *Invest Ophthalmol Vis Sci.* 2007;48:1312–1318.
5. Seeliger M, Kretschmann U, Apfelstedt-Sylla E, Ruther K, Zrenner E. Multifocal electroretinography in retinitis pigmentosa. *Am J Ophthalmol.* 1998;125:214–226.
6. Hood DC, Holopigian K, Greenstein V, et al. Assessment of local retinal function in patients with retinitis pigmentosa using the multi-focal ERG technique. *Vision Res.* 1998;38:163–179.
7. Seeliger MW, Zrenner E, Apfelstedt-Sylla E, Jaissle GB. Identification of Usher syndrome subtypes by ERG implicit time. *Invest Ophthalmol Vis Sci.* 2001;42:3066–3071.
8. Sutter EE, Tran D. The field topography of ERG components in man–I. The photopic luminance response. *Vision Res.* 1992;32:433–446.
9. Nagy D, Schonfisch B, Zrenner E, Jagle H. Long-term follow-up of retinitis pigmentosa patients with multifocal electroretinography. *Invest Ophthalmol Vis Sci.* 2008;49:4664–4671.
10. Hood DC. Assessing retinal function with the multifocal technique. *Prog Retin Eye Res.* 2000;19:607–646.
11. Hood DC, Zhang X. Multifocal ERG and VEP responses and visual fields: comparing disease-related changes. *Doc Ophthalmol.* 2000;100:115–137.

12. Holopigian K, Seiple W, Greenstein VC, Hood DC, Carr RE. Local cone and rod system function in patients with retinitis pigmentosa. *Invest Ophthalmol Vis Sci.* 2001;42:779–788.
13. Robson AG, Saihan Z, Jenkins SA, et al. Functional characterisation and serial imaging of abnormal fundus autofluorescence in patients with retinitis pigmentosa and normal visual acuity. *Br J Ophthalmol.* 2006;90:472–479.
14. Schatz P, Abrahamson M, Eksandh L, Ponjavic V, Andreasson S. Macular appearance by means of OCT and electrophysiology in members of two families with different mutations in RDS (the peripherin/RDS gene). *Acta Ophthalmol Scand.* 2003;81:500–507.
15. Sugita T, Kondo M, Piao CH, Ito Y, Terasaki H. Correlation between macular volume and focal macular electroretinogram in patients with retinitis pigmentosa. *Invest Ophthalmol Vis Sci.* 2008;49:3551–3558.
16. Jacobson SG, Roman AJ, Aleman TS, et al. Normal central retinal function and structure preserved in retinitis pigmentosa. *Invest Ophthalmol Vis Sci.* 2010;51:1079–1085.
17. Rangaswamy NV, Patel HM, Locke KG, Hood DC, Birch DG. A comparison of visual field sensitivity to photoreceptor thickness in retinitis pigmentosa. *Invest Ophthalmol Vis Sci.* 2010;51:4213–4219.
18. Beck RW, Moke PS, Turpin AH, et al. A computerized method of visual acuity testing: adaptation of the early treatment of diabetic retinopathy study testing protocol. *Am J Ophthalmol.* 2003;135:194–205.
19. Marmor MF, Fulton AB, Holder GE, Miyake Y, Brigell M, Bach M. ISCEV Standard for full-field clinical electroretinography (2008 update). *Doc Ophthalmol.* 2009;118:69–77.
20. Hood DC, Wladis EJ, Shady S, Holopigian K, Li J, Seiple W. Multifocal rod electroretinograms. *Invest Ophthalmol Vis Sci.* 1998;39:1152–1162.
21. Birch DG, Williams PD, Callanan D, Wang R, Locke KG, Hood DC. Macular atrophy in birdshot retinochoroidopathy: an optical coherence tomography and multifocal electroretinography analysis. *Retina.* 2010;30:930–937.
22. Dale EA, Hood DC, Greenstein VC, Odel JG. A comparison of multifocal ERG and frequency domain OCT changes in patients with abnormalities of the retina. *Doc Ophthalmol.* 2010;120:175–186.
23. Hood DC, Bach M, Brigell M, et al. ISCEV guidelines for clinical multifocal electroretinography (2007 edition). *Doc Ophthalmol.* 2008;116:1–11.
24. Hood DC, Lin CE, Lazow MA, Locke KG, Zhang X, Birch DG. Thickness of receptor and post-receptor retinal layers in patients with retinitis pigmentosa measured with frequency-domain optical coherence tomography. *Invest Ophthalmol Vis Sci.* 2009;50:2328–2336.
25. Hood DC, Lazow MA, Locke KG, Greenstein VC, Birch DG. The transition zone between healthy and diseased retina in patients with retinitis pigmentosa. *Invest Ophthalmol Vis Sci.* 2011;52:101–108.
26. Birch DG, Anderson JL, Fish GE. Yearly rates of rod and cone functional loss in retinitis pigmentosa and cone-rod dystrophy. *Ophthalmology.* 1999;106:258–268.
27. Curcio CA, Messinger JD, Sloan KR, Mitra A, McGwin G, Spaide RF. Human chorioretinal layer thicknesses measured using macula-wide high resolution histological sections. *Invest Ophthalmol Vis Sci.* 2011;52:3943–54.
28. Robson AG, Michaelides M, Saihan Z, et al. Functional characteristics of patients with retinal dystrophy that manifest abnormal parafoveal annuli of high density fundus autofluorescence; a review and update. *Doc Ophthalmol.* 2008;116:79–89.
29. Hood DC, Seiple W, Holopigian K, Greenstein V. A comparison of the components of the multifocal and full-field ERGs. *Vis Neurosci.* 1997;14:533–544.
30. Greenstein VC, Holopigian K, Seiple W, Carr RE, Hood DC. Atypical multifocal ERG responses in patients with diseases affecting the photoreceptors. *Vision Res.* 2004;44:2867–2874.